

NASA TECHNICAL NOTE



NASA TN D-3035

C. 1

LOAN COPY: RE  
AFWL (WL)  
BIRTLAND AFB



NASA TN D-3035

AERODYNAMIC CHARACTERISTICS IN PITCH  
OF SEVERAL M-WING—BODY COMBINATIONS  
AT MACH NUMBERS OF 2.40, 2.60, AND 2.86

*by Odell A. Morris and F. Edward McLean*

*Langley Research Center*

*Langley Station, Hampton, Va.*



# AERODYNAMIC CHARACTERISTICS IN PITCH OF SEVERAL

## M-WING—BODY COMBINATIONS AT MACH NUMBERS

OF 2.40, 2.60, AND 2.86

By Odell A. Morris and F. Edward McLean  
Langley Research Center

### SUMMARY

An investigation has been made in the Langley Unitary Plan wind tunnel at Mach numbers of 2.40, 2.60, and 2.86 to determine the longitudinal aerodynamic characteristics of several M-wing—body configurations. The M-wing planforms had  $76^\circ$  leading-edge sweep angles on the outer wing panels and the investigation included both a flat wing and a twisted and cambered wing designed for a Mach number of 2.60 and a lift coefficient of 0.0625. Each wing had streamwise 2.5-percent-thick circular-arc wing sections and an aspect ratio of 1.71. The bodies had circular cross-sectional shapes, and the models were tested with two body nose lengths. The results have been compared with those from tests of a similar wing-body combination having an arrow-wing planform.

The M-wing planform provided a considerable improvement in pitching-moment linearity over that obtained with the arrow-wing planform for both the flat and the warped wings. The flat M-wing model indicated maximum values of lift-drag ratio that were slightly higher than those obtained for the flat arrow-wing model at a Mach number of 2.40 but somewhat lower at Mach numbers of 2.60 and 2.86. The warped M-wing model generally showed only slightly higher maximum values of lift-drag ratio than the flat M-wing model but did provide positive values of pitching moment at zero lift which would improve the longitudinal trim characteristics. The warped M-wing model had lower maximum values of lift-drag ratio than the warped arrow-wing model at each test Mach number due to a higher minimum drag level and a higher drag due to lift.

### INTRODUCTION

The National Aeronautics and Space Administration has an intensive research program underway to provide the research background necessary to define and meet design requirements for a commercially acceptable supersonic transport aircraft. As a part of this program a number of investigations have recently been made on highly swept twisted and cambered arrow wings in an effort to obtain improved lift-drag ratios. (See refs. 1 to 4, for example.) These studies indicate

that the twisted and cambered arrow-wing planform showed considerable improvement in lift-drag values over a comparable flat wing. However, in the subsonic speed range, tests have shown that the highly swept arrow-wing planform has an undesirable pitch-up tendency (ref. 5).

A number of investigations have been made in the subsonic and transonic speed ranges on M-wing planforms (see refs. 6 to 9) which exhibited substantially better pitching-moment linearity than exhibited by the equivalent swept-wing planforms. The subsonic and transonic tests did not include any highly swept M-shape wings, however, and heretofore no data have been available on highly swept M-shape wing planforms in the supersonic speed range.

Therefore, the present investigation was conducted using two M-wing model configurations which have planforms identical to the  $76^\circ$  swept arrow wing of reference 3, except that the inboard section of the wing has been swept rearward to form an M-shape planform. Tests of the two wing-body configurations have been conducted at Mach numbers of 2.40, 2.60, and 2.86 over an angle-of-attack range of about  $-4^\circ$  to  $6^\circ$ , and at a Reynolds number of  $3.0 \times 10^6$  per foot. The results of the investigation have been compared with results of tests of the  $76^\circ$  swept arrow-wing planform of reference 3 and are presented herein with a limited analysis.

#### SYMBOLS

The results are referred to the stability-axis system with the moment reference point located at a station corresponding to the quarter-chord point of the wing mean aerodynamic chord as shown in figure 1.

$C_D$	drag coefficient, Drag/ $qS$
$C_L$	lift coefficient, Lift/ $qS$
$C_m$	pitching-moment coefficient, Pitching moment/ $qS\bar{c}$
$\bar{c}$	mean aerodynamic chord
$L/D$	lift-drag ratio
$M$	free-stream Mach number
$q$	free-stream dynamic pressure, lb/sq ft
$r$	radial coordinate
$S$	reference wing area
$x$	chordwise distance measured from fuselage nose
$x'$	chordwise distance measured from wing apex

y            spanwise distance measured from fuselage center line  
z<sub>c</sub>          vertical distance measured from wing reference plane  
 $\alpha$         angle of attack, deg

Model component designations:

B<sub>s</sub>          short-nose body  
B<sub>L</sub>          long-nose body  
M-W<sub>f</sub>       flat M-wing  
M-W<sub>w</sub>       warped M-wing  
A-W<sub>f</sub>       flat arrow wing  
A-W<sub>w</sub>       warped arrow wing

## MODELS AND APPARATUS

Two wing-body models were considered in the present investigation. Both models had identical body shapes and wing planforms, except that one model had a flat wing and the other a twisted and cambered wing which was designed for a Mach number of 2.60 and lift coefficient of 0.0625. Details of the model with the flat wing are shown in figure 1. Photographs are shown in figure 2 for the flat wing model and the warped wing model. Coordinates for the warped wing model are given in table I. The M-shape wing planforms had streamwise 2.5-percent-thick circular-arc wing sections and an aspect ratio of 1.71. The leading edge of the outboard wing panel was swept back  $76^\circ$  with the apexes located at 31.25 percent of the wing semispan. The leading edge of the inboard panel was swept back  $67.4^\circ$ .

The body had circular cross-sectional shapes for which the coordinates are listed in table II. The body was constructed with a removable nose section so that the body length could be extended by adding an 8-inch cylindrical body section as shown in figure 1.

The wing-body models, which were cast of brass, were sting-mounted from the tunnel central support system and the forces and moments were measured by means of a six-component strain-gage balance mounted within the model.

## TESTS, CORRECTIONS, AND ACCURACY

The investigation was conducted in the Langley Unitary Plan wind tunnel at the following test conditions:

Mach number . . . . .	2.40	2.60	2.86
Reynolds number (based on $\bar{c}$ ) . . . . .	$3.5 \times 10^6$	$3.5 \times 10^6$	$3.5 \times 10^6$
Stagnation pressure, lb/sq ft . . . . .	2405	2680	3075
Stagnation temperature, $^{\circ}\text{F}$ . . . . .	150	150	150

The stagnation dewpoint was maintained sufficiently low to prevent measurable condensation effects in the test section. Test were made through an angle-of-attack range of about  $-4^{\circ}$  to  $6^{\circ}$  for each Mach number. The angles of attack were corrected for the deflection of the balance and sting under load and for tunnel flow angularity. The balance-chamber pressures were measured and the drag forces were adjusted to correspond to a condition of free-stream static pressure at the model base.

In order to assure a turbulent boundary layer, transition strips of No. 120 carborundum grit 1/16 inch wide were located 15/16 inch from the body nose and 1/16 inch from the wing leading edges (measured perpendicular to the leading edge).

Based upon balance accuracy and repeatability of data, it is estimated that the measured quantities are accurate to within the following limits:

$C_L$ . . . . .	$\pm 0.003$
$C_D$ . . . . .	$\pm 0.0005$
$C_m$ . . . . .	$\pm 0.0005$
$\alpha$ , deg . . . . .	$\pm 0.1$
M . . . . .	$\pm 0.015$

## RESULTS AND DISCUSSION

Both the flat and the warped M-wing models were tested with short and long noses in an effort to determine the magnitude of the unfavorable drag interference associated with the impingement of the nose compressions from the short nose on the advancing surfaces of the outboard wing panels. The long-nose body was just long enough to insure that nose compressions would miss the wing entirely. The data of figures 3 and 4 show the effects of nose length, and it is apparent that the increased wetted area of the long-nosed arrangement produces a drag increment which exceeds the unfavorable drag interference associated with the short forebody. As would be expected, the longer nose produced a destabilizing effect.

The data of figure 5 show a comparison of the aerodynamic characteristics in pitch for the flat M-wing model and the flat arrow-wing model of reference 3. The flat arrow-wing model has essentially the same maximum sweep, aspect ratio, and area as the M-wing. However, the M-wing model had a lower leading-edge sweep in the inboard regions. The bodies of the models of reference 3 had the same length and volume as the short-body configurations used in the present tests, but had slightly different body cross-sectional shapes. (For complete model details, see ref. 3.) It is believed that the difference in body

cross-sectional shape between the two models would have a negligible effect on the measured components.

At a Mach number of 2.40, the minimum drags for both models were about the same and the M-wing indicated a slightly higher maximum value of  $L/D$ . However, increasing the Mach number to 2.86 produced larger decreases in minimum drag for the arrow wing than for the M-wing and these decreases resulted in somewhat higher maximum values of  $L/D$  for the arrow-wing model. The higher minimum drag values for the flat M-wing at Mach numbers of 2.60 and 2.86 are associated with the relatively low sweep of the inboard region of the wing and thus resulted in the transition from a subsonic to a supersonic leading edge over that region as Mach number was increased. A comparison of the pitching-moment results (fig. 5(b)) indicates considerably less nonlinearity for the M-wing than for the arrow wing.

Figure 6 shows a comparison of the data for the flat M-wing model, the warped M-wing model, and the warped arrow-wing model of reference 3. The warped M-wing model shows only a small gain in the maximum values of  $L/D$  at each Mach number when compared with the flat M-wing model. However, the warped M-wing model does show a favorable shift in pitching moment at zero lift, similar to that for the warped arrow wing, which would tend to improve the maximum trimmed values of  $L/D$ . As was the case with the flat wings, the warped M-wing indicates a considerable improvement in pitching-moment linearity when compared with the warped arrow wing (fig. 6(b)).

The maximum values of  $L/D$  for the warped M-wing model in comparison with those for the warped arrow wing were lower by about 0.6 at  $M = 2.40$  and about 0.9 at  $M = 2.86$  (fig. 6(d)). This difference in performance is due to both the higher minimum drag and the higher drag due to lift which was obtained for the warped M-wing model (fig. 6(c)). It should be pointed out that for the purpose of the present investigation, no attempt was made to optimize the warped surface of the M-wing model. This fact, together with the somewhat lower sweep angle employed in the inboard region of the M-wing, is believed to be responsible for the higher drag due to lift of this configuration. It would be expected that an analytic solution for the lifting-surface shape and the use of completely subsonic leading edges as indicated by theory (ref. 2) would result in a somewhat better drag-due-to-lift factor for the M-wing planform.

The oil-flow photographs of figure 7 for the warped M-wing model show a strong compression in the forward portions of the wing-body juncture. These compressions would be evident in any such M-wing arrangement but would tend to be relieved as local leading edges were swept farther behind the Mach cone. Such increases in local leading-edge sweep when accompanied by judicious body shaping should reduce the configuration wave drag.

#### SUMMARY OF RESULTS

An investigation has been made in the Langley Unitary Plan wind tunnel to determine the longitudinal aerodynamic characteristics at Mach numbers of 2.40, 2.60, and 2.86 of two M-wing-body models having a flat and a warped wing.

Comparison of the data with those of a similar arrow-wing body configuration reported in reference 3 indicated the following results:

1. The M-wing planform provided a considerable improvement in pitching-moment linearity over that obtained with the arrow-wing planform for both the flat and the warped wings.
2. The flat M-wing model indicated maximum values of lift-drag ratio that were slightly higher than those obtained for the flat arrow-wing model at a Mach number of 2.40 but somewhat lower at Mach numbers of 2.60 and 2.86.
3. The warped M-wing model indicated only slightly higher values of maximum lift-drag ratio than the flat M-wing model but did provide positive values of pitching moment at zero lift which would improve the longitudinal trim characteristics.
4. The warped M-wing model had lower maximum values of lift-drag ratio than the warped arrow-wing model at each test Mach number due to a higher minimum drag level and a higher drag due to lift.

Langley Research Center,  
National Aeronautics and Space Administration,  
Langley Station, Hampton, Va., May 10, 1965.

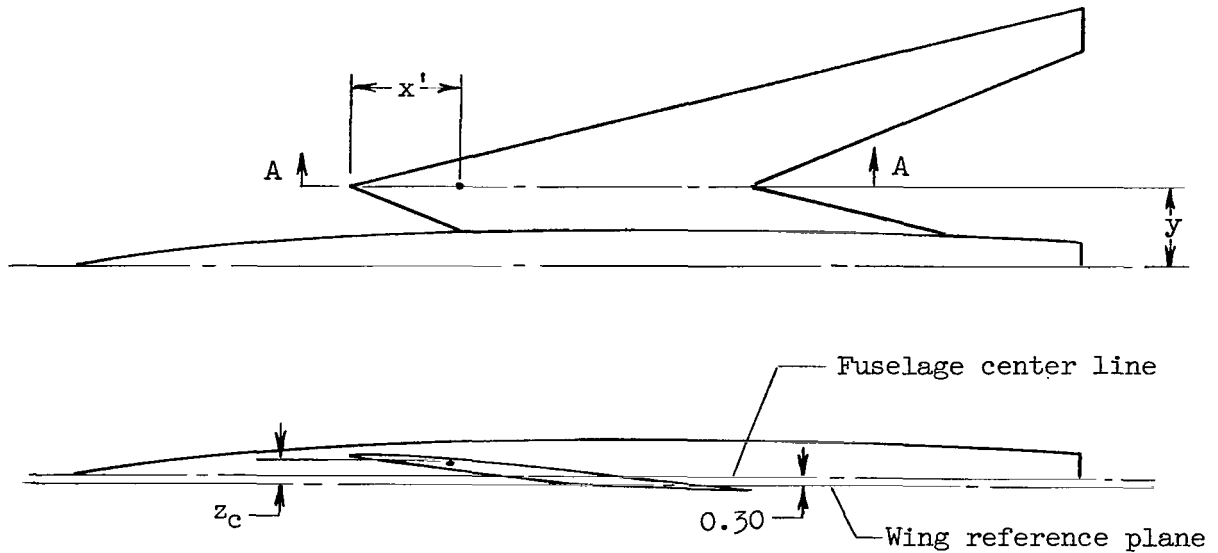
## REFERENCES

1. Carlson, Harry W.: Aerodynamic Characteristics at Mach Number 2.05 of a Series of Highly Swept Arrow Wings Employing Various Degrees of Twist and Camber. NASA TM X-332, 1960.
2. Brown, Clinton E.; and McLean, Francis E.: The Problem of Obtaining High Lift-Drag Ratios at Supersonic Speeds. J. Aero/Space Sci., vol. 26, no. 5, May 1959, pp. 298-302.
3. McLean, F. Edward; and Fuller, Dennis E.: Effects of Thickness on Supersonic Performance of a Wing-Body Configuration Employing a Warped Highly Swept Arrow Wing. NASA TN D-3034, 1965.
4. Morris, Odell A.; and Robins, A. Warner: Aerodynamic Characteristics at Mach Number 2.01 of an Airplane Configuration Having a Cambered and Twisted Arrow Wing Designed for a Mach Number of 3.0. NASA TM X-115, 1959.
5. Lockwood, Vernard E.; McKinney, Linwood W.; and Lamar, John E.: Low-Speed Aerodynamic Characteristics of a Supersonic Transport Model With a High-Aspect-Ratio Variable-Sweep Warped Wing. NASA TM X-979, 1964.
6. Fournier, Paul G.: Effects of Spanwise Location of Sweep Discontinuity on the Low-Speed Longitudinal Stability Characteristics of a Complete Model With Wings of M and W Plan Form. NACA RM L54K23, 1955.
7. Kemp, William B., Jr.: Aerodynamic Characteristics at Small Scale and a Mach Number of 1.38 of Untapered Wings Having M and W Plan Forms. NACA RM L54D15a, 1954.
8. Loving, Donald L.: Investigation of the Effect of Indentation on an M-Plan-Form-Wing—Body Combination at Transonic Speeds. NACA RM L54F14, 1954.
9. Weil, Joseph; and Polhamus, Edward C.: Aerodynamic Characteristics of Wings Designed for Structural Improvement. NACA RM L51E10a, 1951.



TABLE I.- CAMBER SURFACE ORDINATES FOR WARPED WING MODEL

[All dimensions are in inches]



$x' = 0.0$	
$y$	$z_c$
3.125	0.696

$x' = 2.75$	
$y$	$z_c$
1.979	0.569
2.000	.572
2.200	.586
2.400	.593
2.600	.586
2.800	.575
3.000	.555
3.125	.539
3.200	.555
3.300	.568
3.400	.582
3.500	.591
3.600	.592
3.700	.583
3.800	.550
3.812	.542

$x' = 5.5$	
$y$	$z_c$
0.833	0.442
1.000	.460
1.400	.580
1.800	.473
2.000	.467
2.200	.452
2.400	.435
2.600	.416
2.800	.395
3.000	.372
3.125	.358
3.200	.370
3.400	.410
3.600	.445
3.800	.475
4.000	.484
4.200	.475
4.400	.438
4.500	.395

TABLE I.- CAMBER SURFACE ORDINATES FOR WARPED WING MODEL - Concluded

$x' = 8.25$	
$y$	$z_c$
0	0.348
.400	.373
.800	.380
1.200	.373
1.600	.356
2.000	.330
2.400	.300
2.600	.282
2.800	.262
3.000	.242
3.125	.232
3.200	.245
3.500	.294
3.800	.334
4.100	.364
4.400	.379
4.700	.374
5.000	.332
5.188	.264

$x' = 11.00$	
$y$	$z_c$
0	0.333
.400	.340
.800	.339
1.200	.325
1.600	.300
2.000	.267
2.400	.231
2.600	.210
2.800	.190
3.000	.168
3.125	.150
3.200	.163
3.600	.195
4.000	.228
4.400	.255
4.800	.279
5.200	.280
5.600	.233
5.750	.195
5.875	.146

$x' = 13.75$	
$y$	$z_c$
0	0.319
.400	.321
.800	.318
1.200	.302
1.600	.279
2.000	.244
2.400	.206
2.600	.188
2.800	.166
3.000	.146
3.125	.136
3.200	.137
3.700	.145
4.200	.157
4.600	.166
5.000	.179
5.400	.186
5.800	.189
6.200	.160
6.400	.130
6.560	.094

$x' = 16.5$	
$y$	$z_c$
0	0.305
.40	.307
.80	.299
1.20	.283
1.60	.258
2.00	.223
2.40	.186
2.60	.166
2.75	.151
3.75	.118
4.00	.117
4.50	.115
5.00	.113
5.50	.113
6.00	.121
6.50	.135
7.00	.155
7.15	.140
7.25	.110

$x' = 19.25$	
$y$	$z_c$
0	0.291
.40	.293
.80	.279
1.20	.255
1.60	.219
1.80	.199
2.06	.176
4.90	.086
5.00	.084
5.40	.081
5.80	.081
6.20	.085
6.60	.100
7.00	.141
7.40	.174
7.80	.158
7.93	.124

$x' = 22$	
$y$	$z_c$
0	0.278
.300	.280
.600	.275
.900	.252
1.200	.223
1.380	.200
6.042	.075
6.400	.066
6.800	.070
7.200	.100
7.600	.147
7.800	.179
8.000	.188
8.333	.186
8.400	.183
8.450	.180
8.500	.172
8.600	.147
8.625	.138

$x' = 24.75$	
$y$	$z_c$
0	0.264
.100	.270
.200	.273
.300	.275
.400	.268
.500	.258
.600	.242
.688	.225
7.188	.065
7.600	.106
7.800	.126
8.000	.154
8.333	.186
8.500	.197
8.700	.210
8.800	.206
9.000	.206
9.200	.185
9.313	.149

$x' = 27.5$	
$y$	$z_c$
8.333	0.150
8.600	.175
8.900	.195
9.450	.223
9.588	.223
9.725	.212
9.863	.188
10.000	.160

TABLE II.- BODY COORDINATES

[All dimensions are in inches]

Body station, x	Body radius, r
0	0
2	.370
4	.635
6	.841
8	1.021
10	1.165
12	1.260
14	1.310
16	1.310
18	1.310
20	1.310
22	1.310
24	1.310
26	1.310
28	1.310
30	1.310
32	1.310
34	1.277
36	1.137
38	1.000

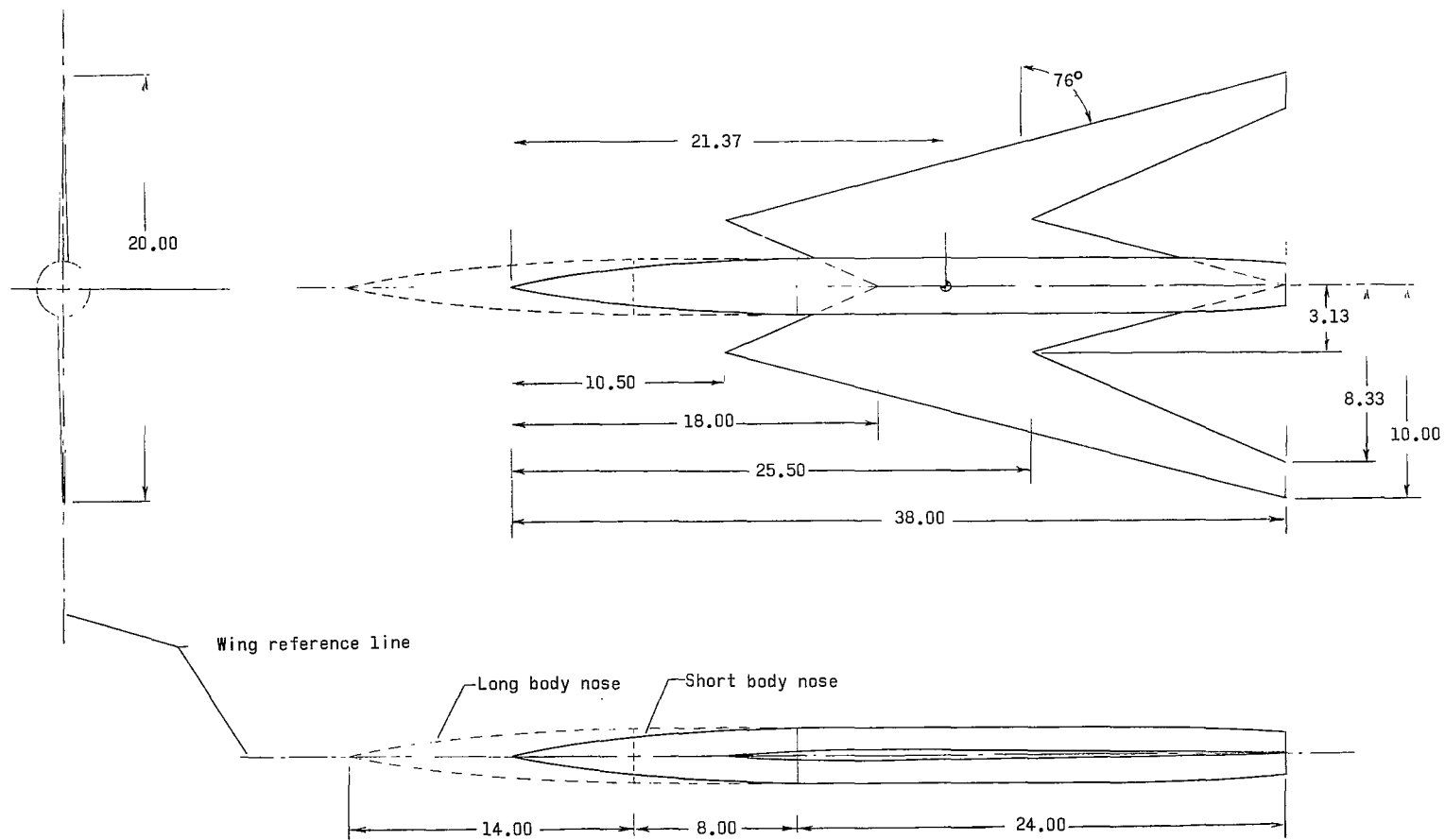
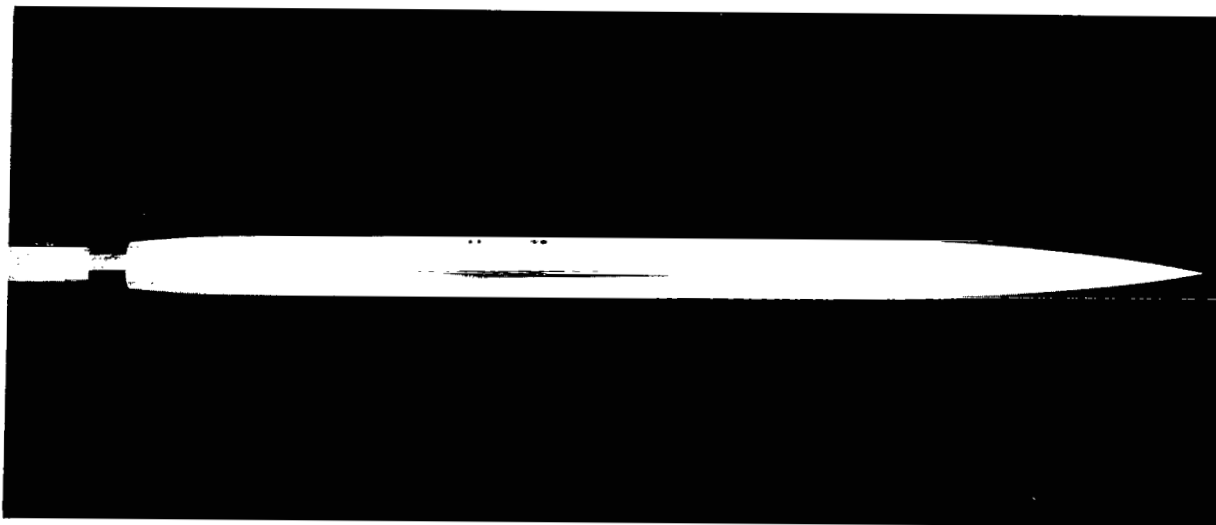
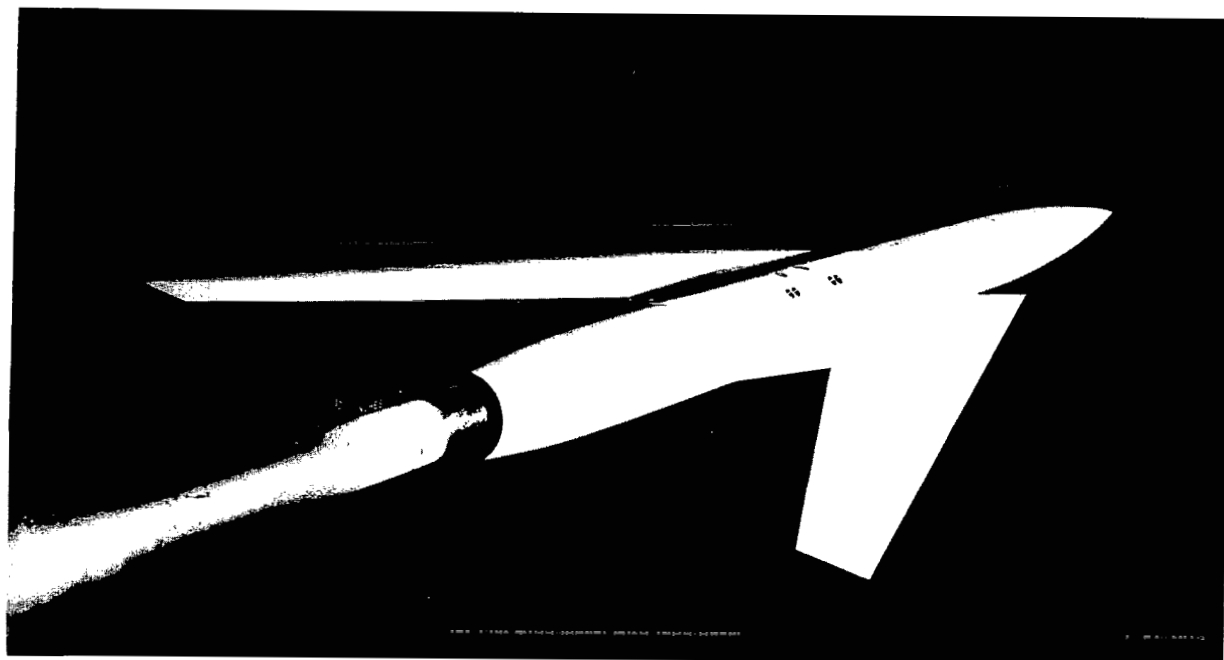


Figure 1.- Details of models, flat wing shown. All dimensions are in inches unless otherwise specified.



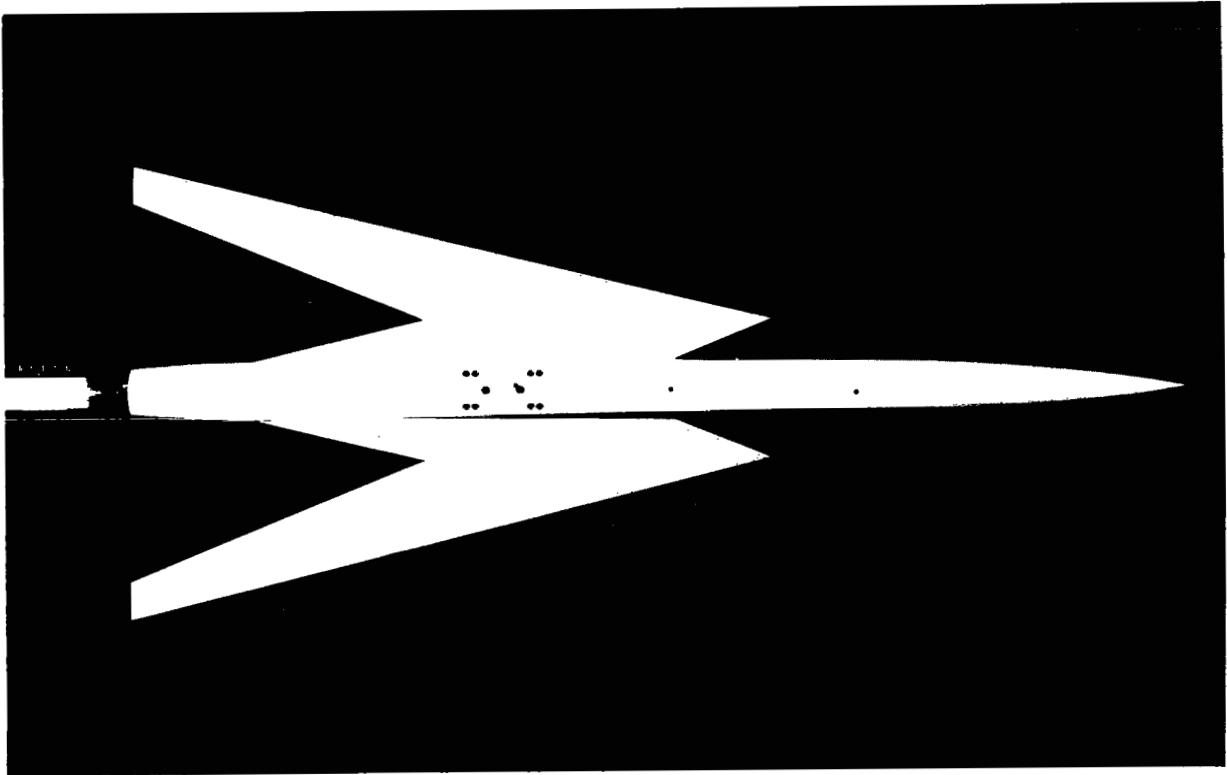
L-63-7818



(a) Flat wing model with long nose.

L-63-7815

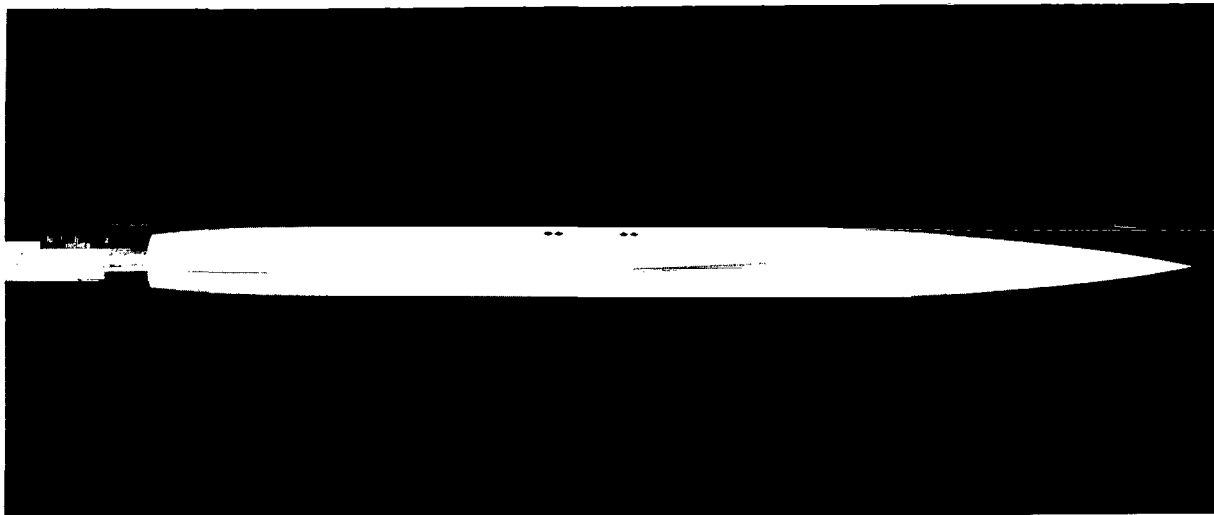
Figure 2- Photographs of models.



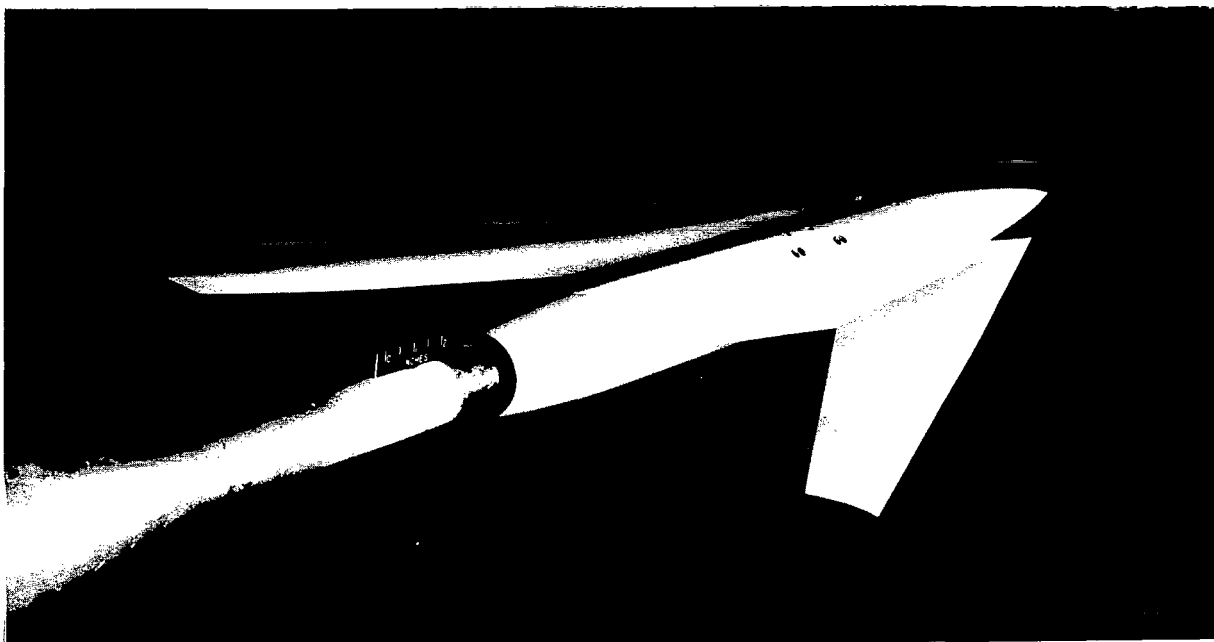
(a) Concluded.

L-63-7817

Figure 2.- Continued.



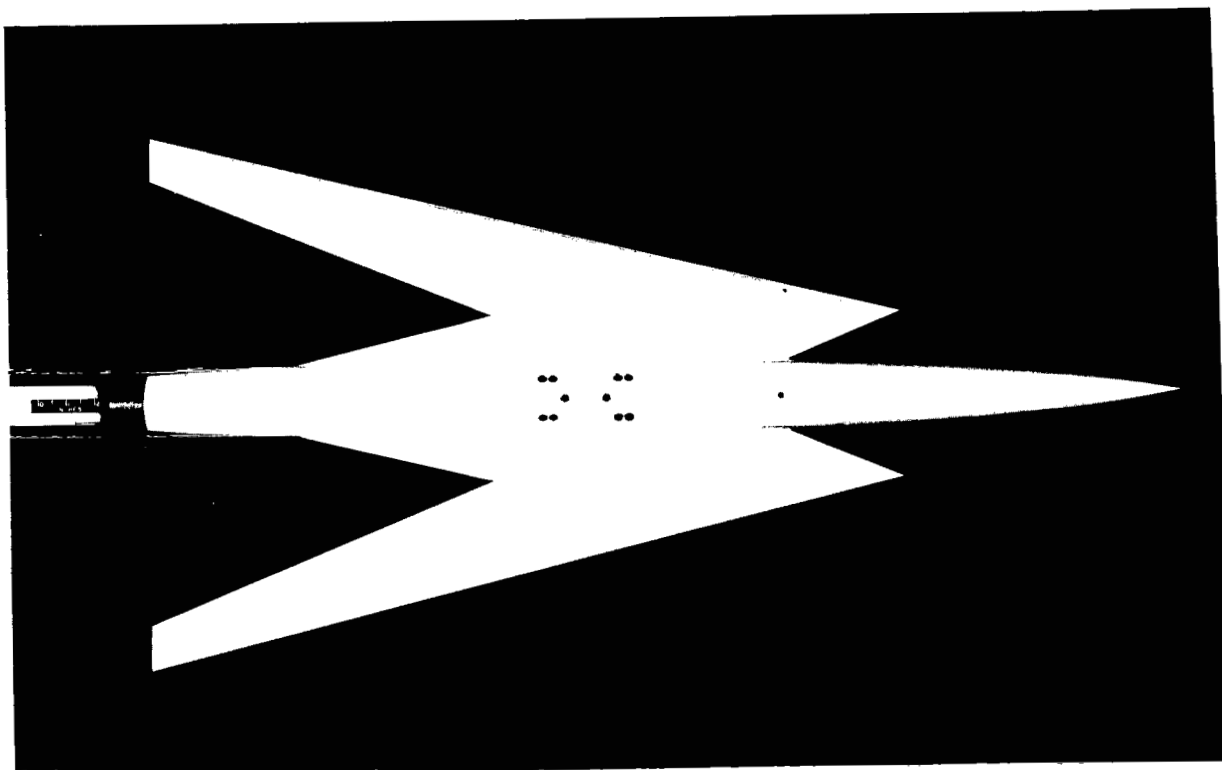
L-63-7812



(b) Warped wing model with short nose.

L-63-7814

Figure 2- Continued.



(b) Concluded.

L-63-7816

Figure 2- Concluded.



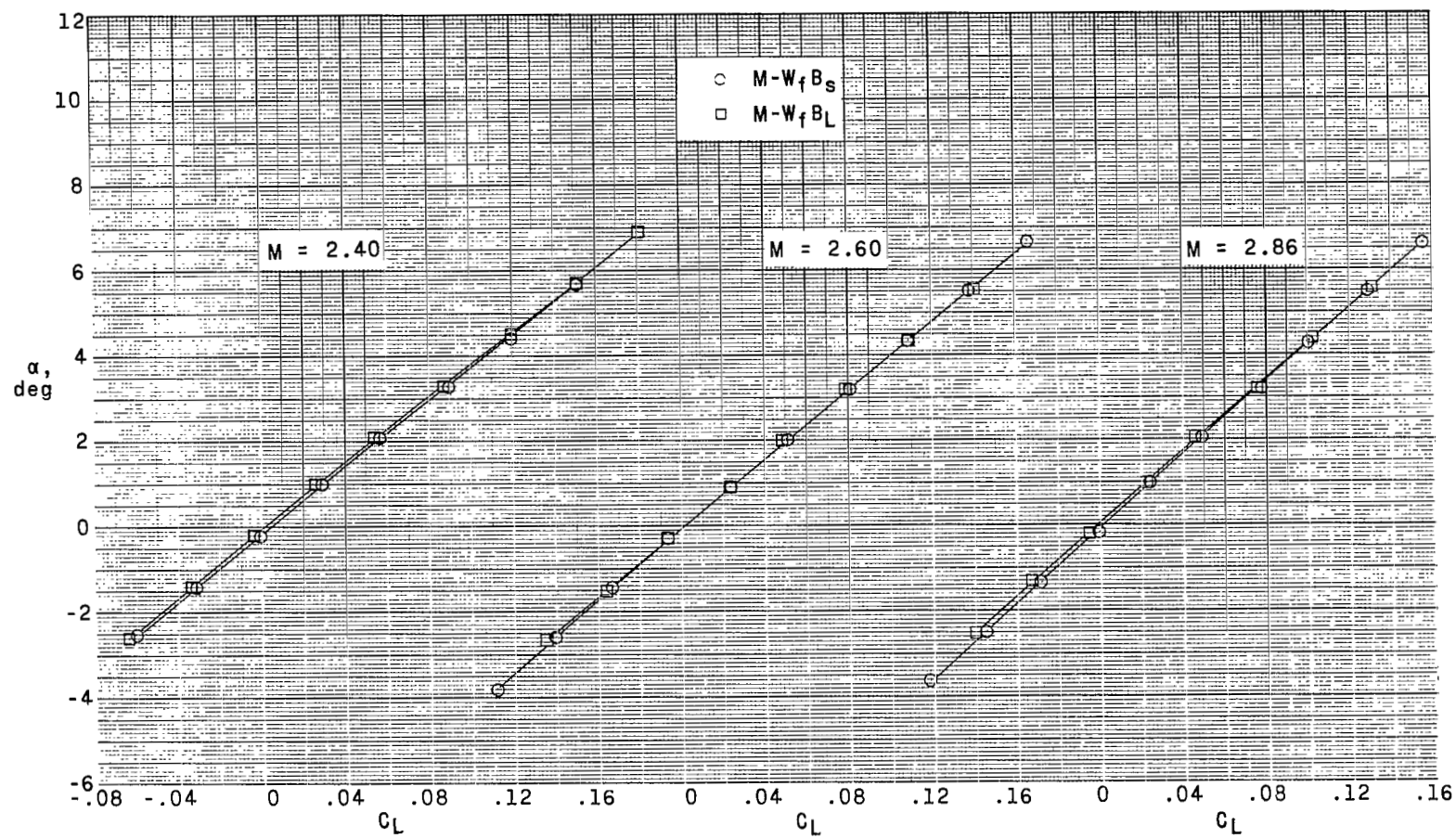
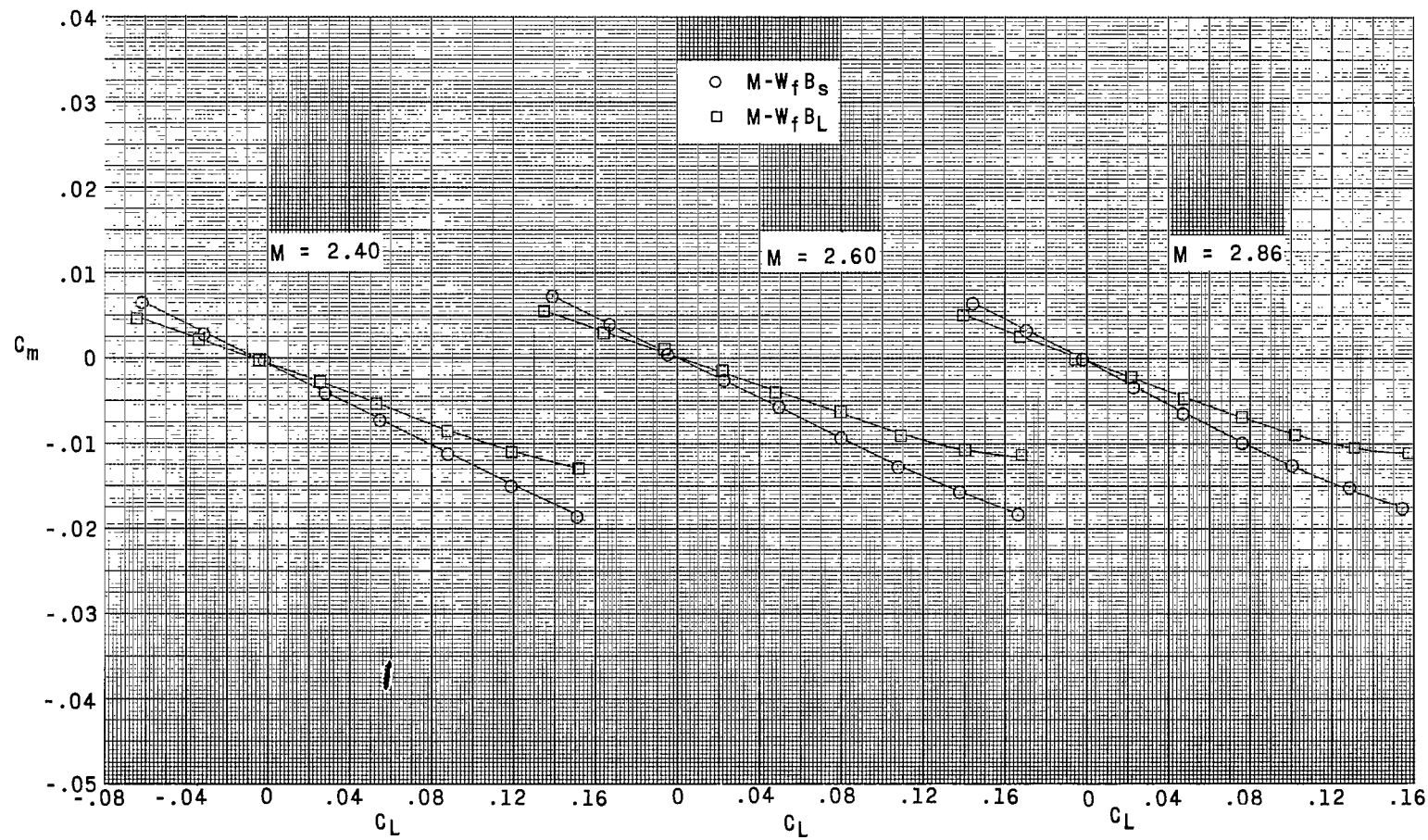
(a) Variation of  $\alpha$  with  $C_L$ .

Figure 3.- Aerodynamic characteristics in pitch for the flat M-wing model with both the short and long body nose.



(b) Variation of  $C_m$  with  $C_L$ .

Figure 3.- Continued.

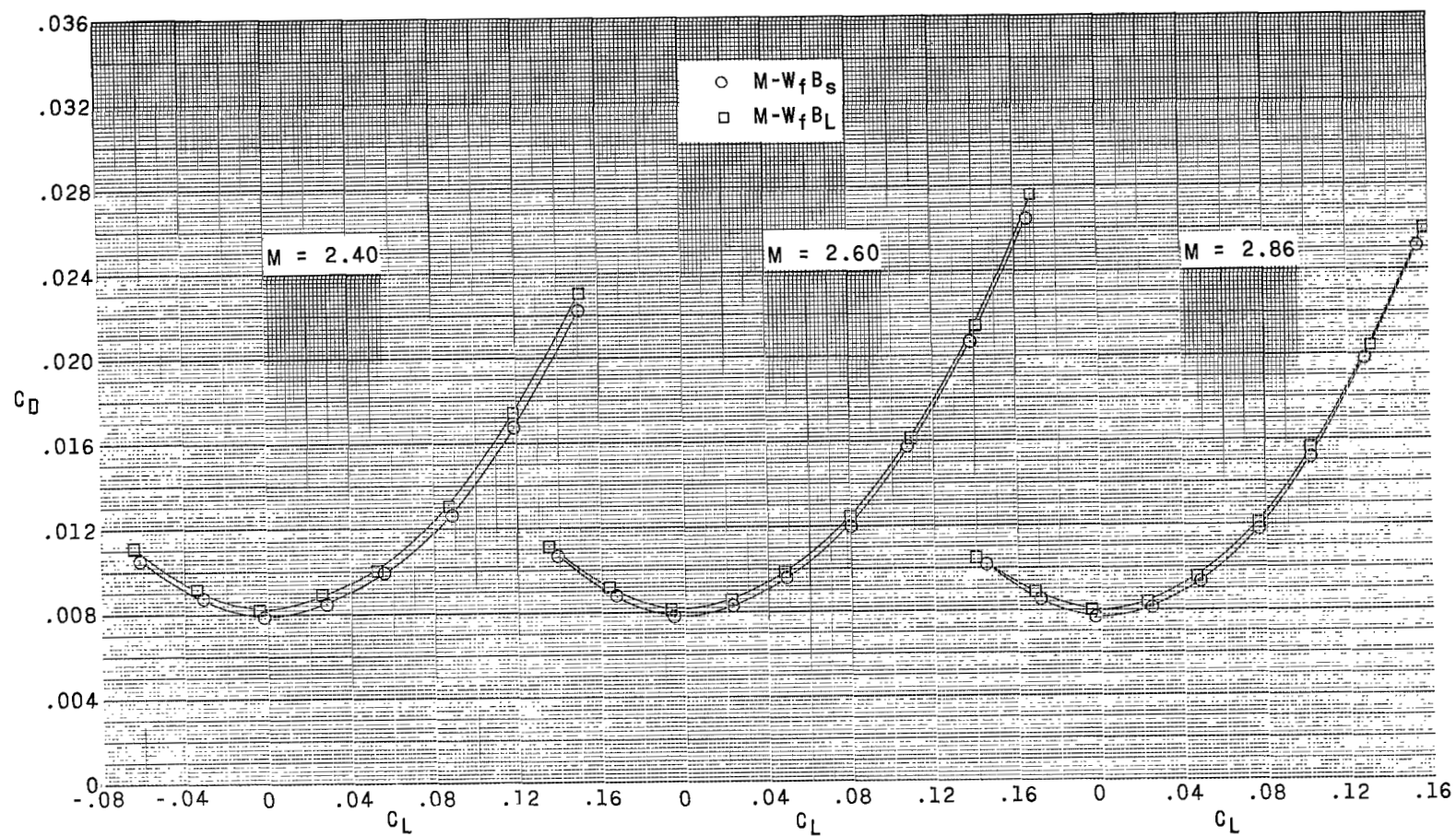
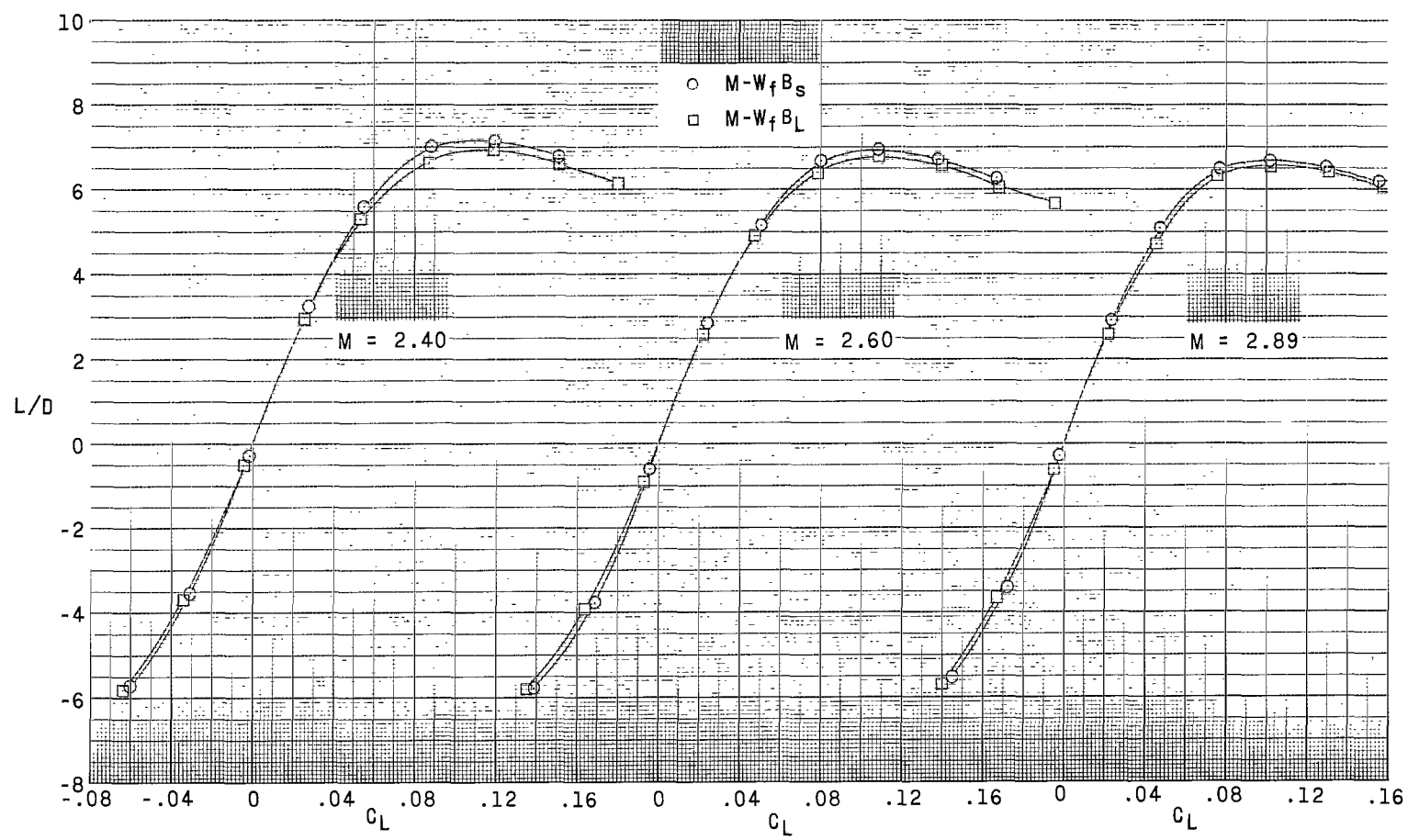
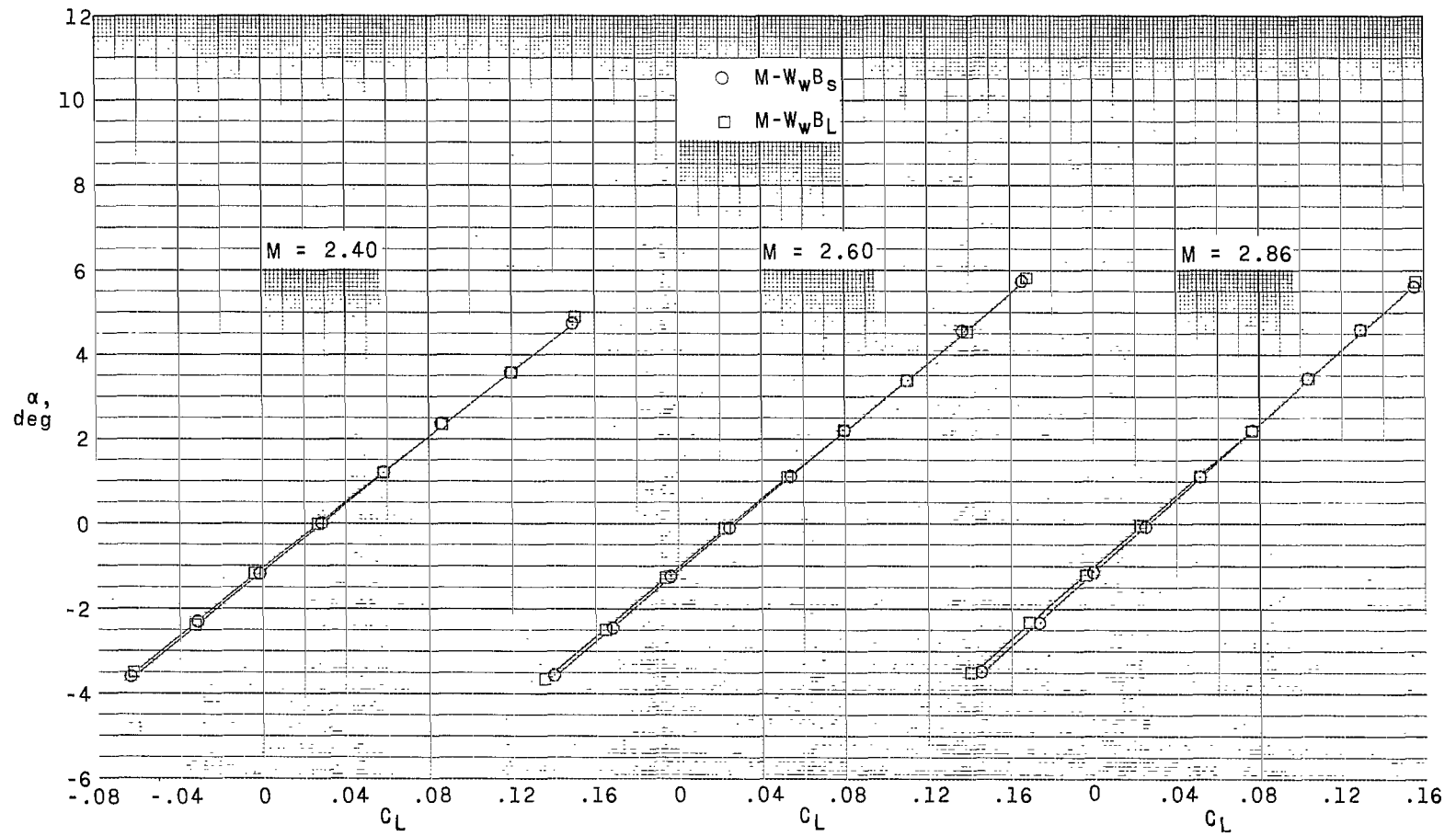
(c) Variation of  $C_D$  with  $C_L$ .

Figure 3.- Continued.



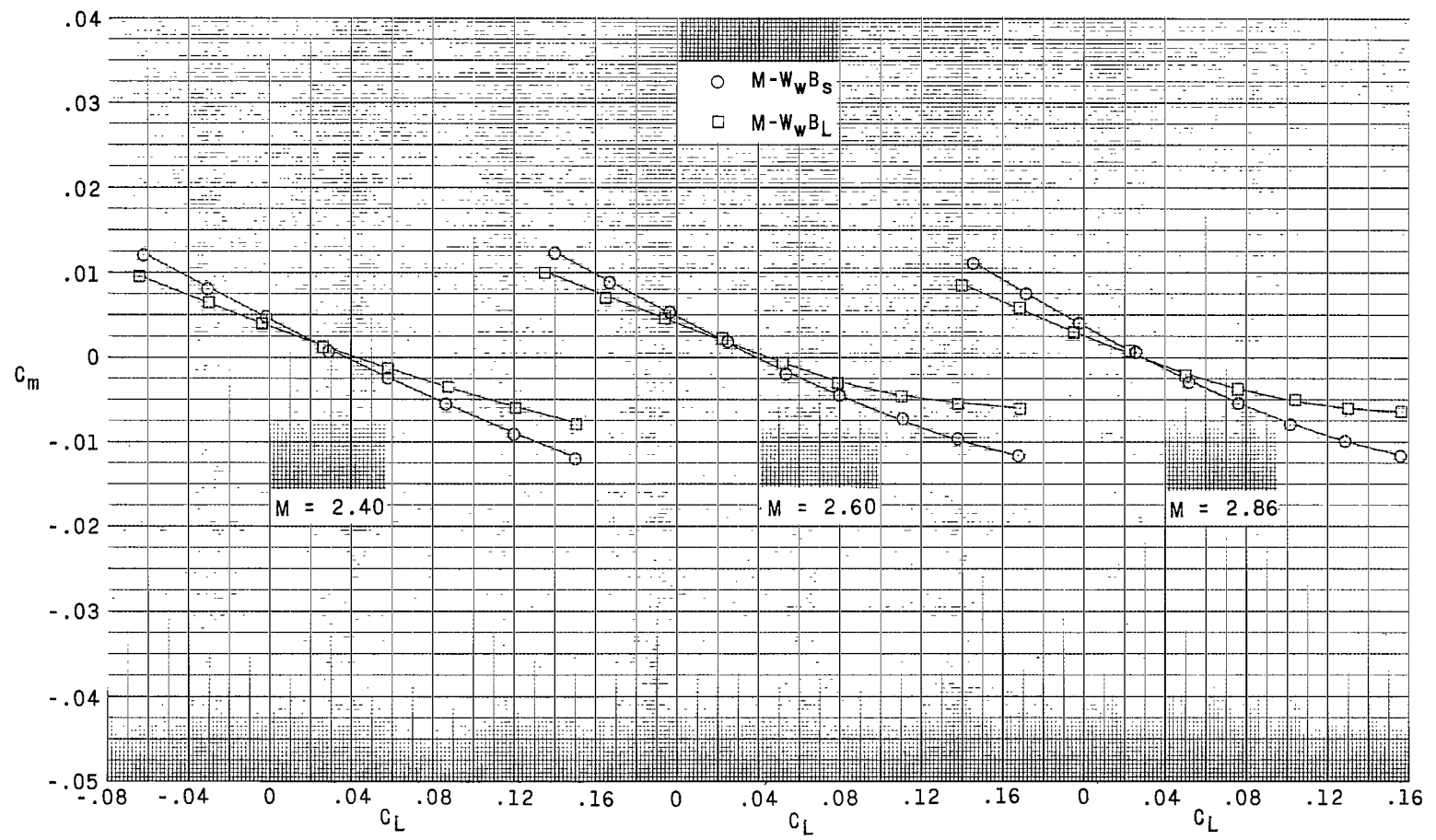
(d) Variation of  $L/D$  with  $C_L$ .

Figure 3.- Concluded.



(a) Variation of  $\alpha$  with  $C_L$ .

Figure 4.- Aerodynamic characteristics in pitch for the warped M-wing model with both the short and long body nose.



(b) Variation of  $C_m$  with  $C_L$ .

Figure 4.- Continued.

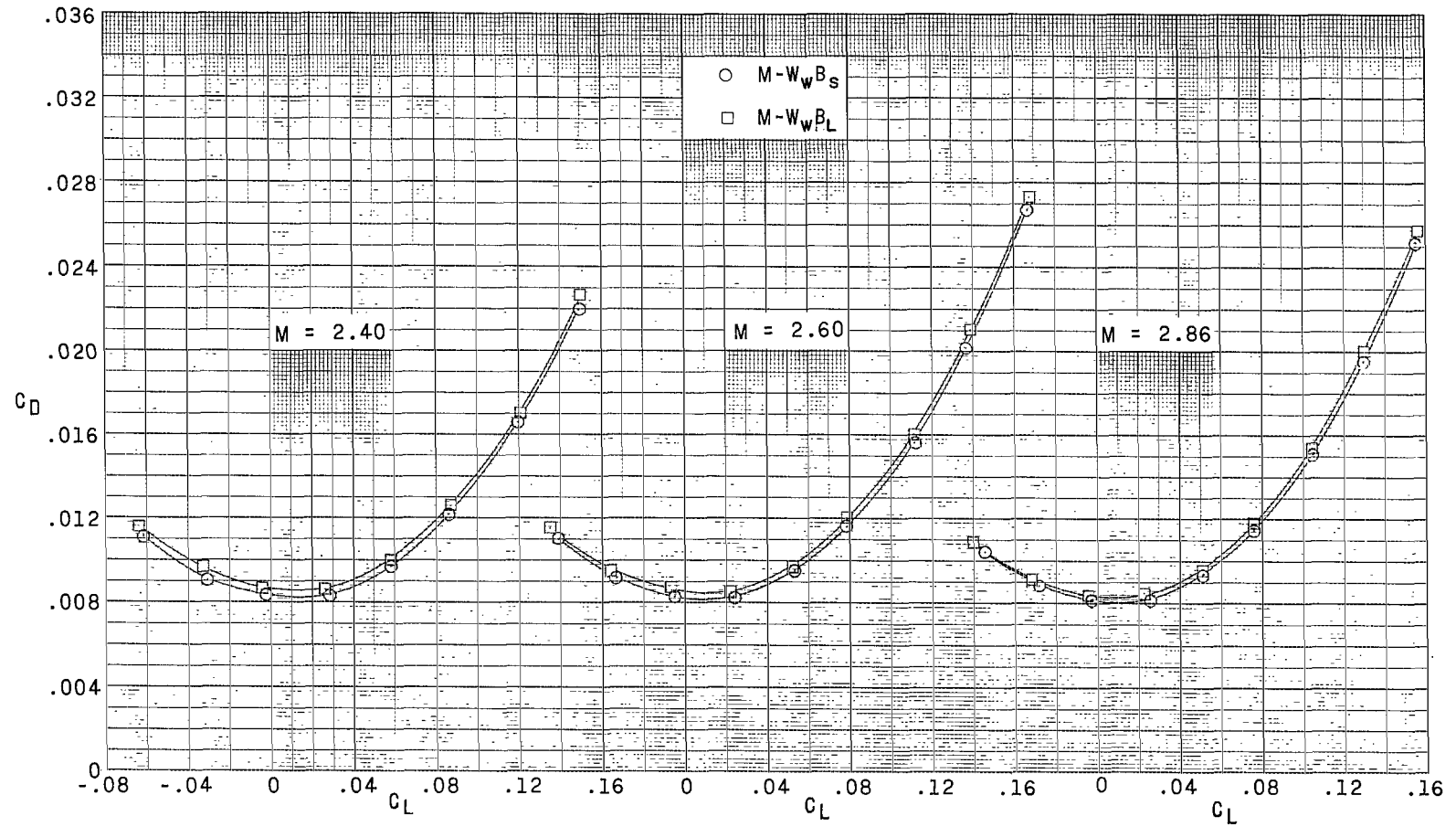
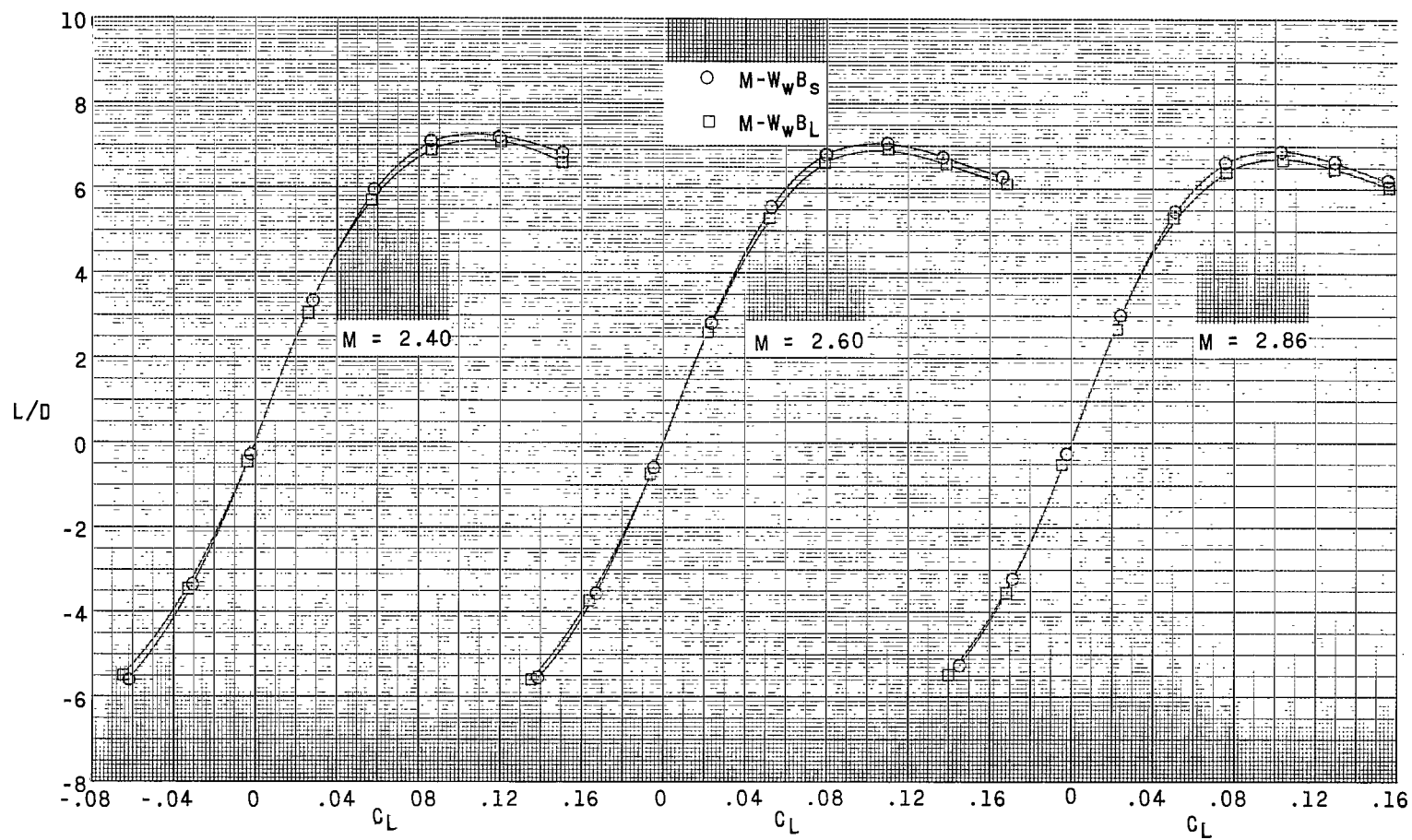
(c) Variation of  $C_D$  with  $C_L$ .

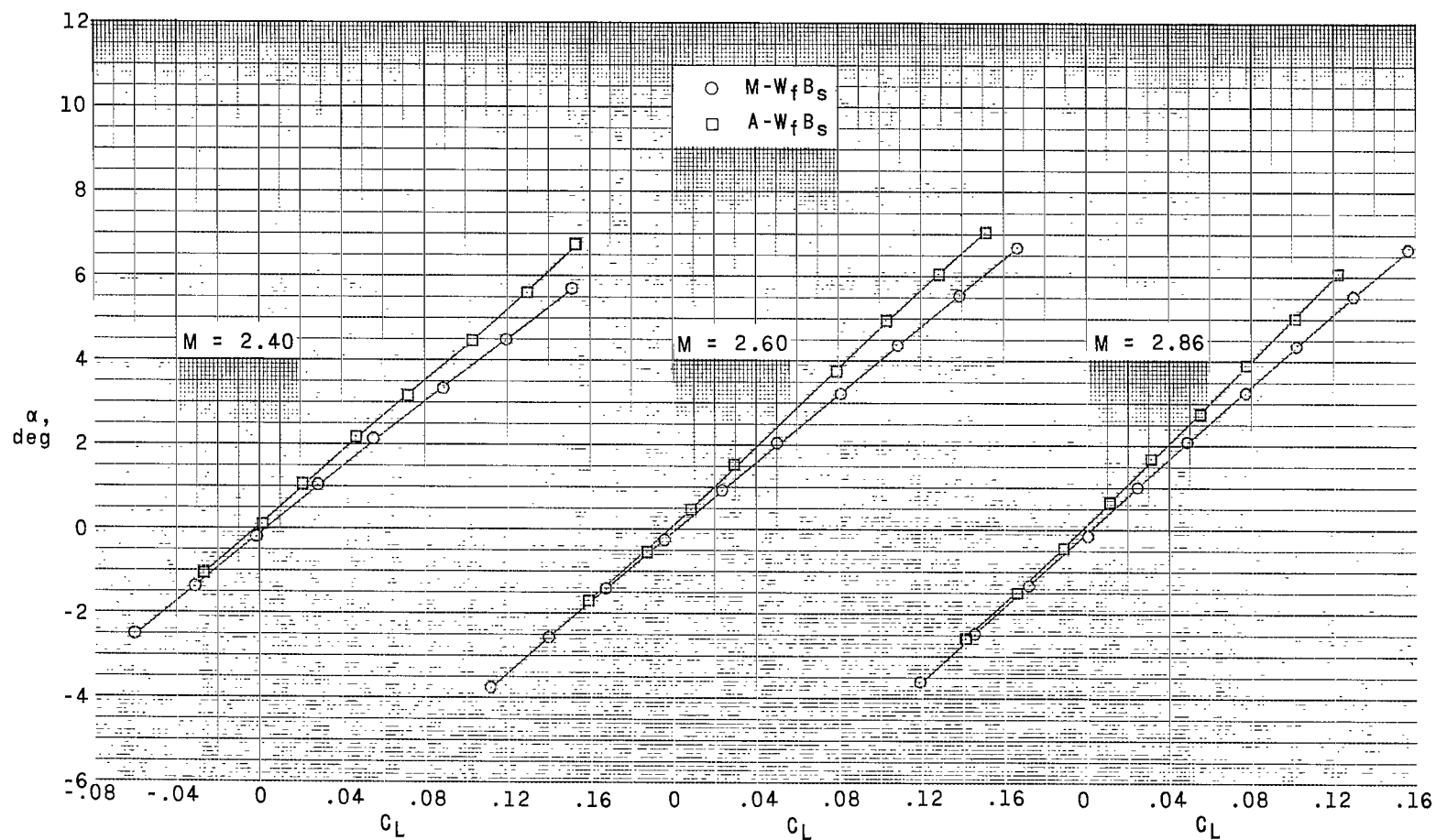
Figure 4.- Continued.



(d) Variation of  $L/D$  with  $C_L$ .

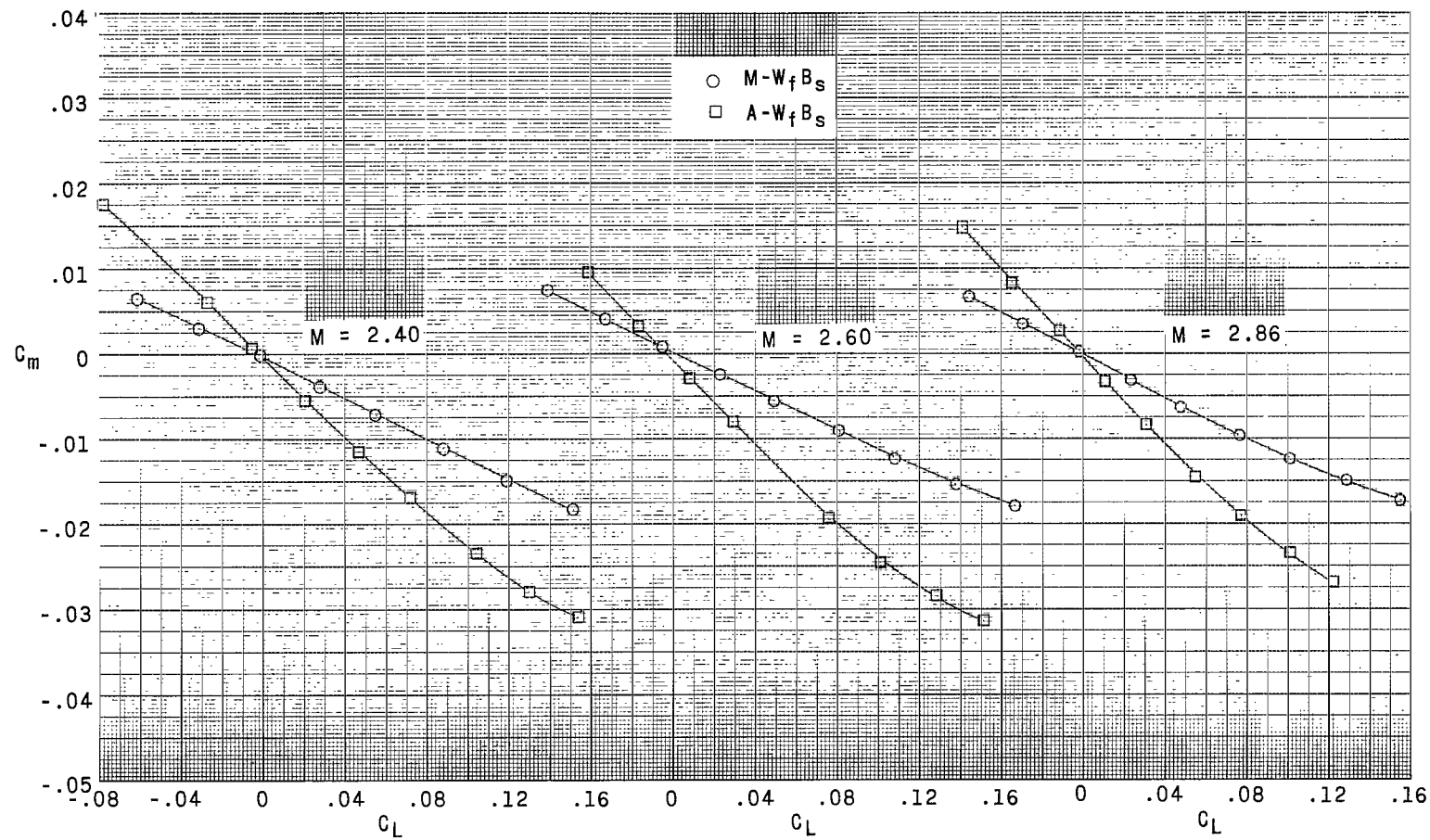
Figure 4.- Concluded.





(a) Variation of  $\alpha$  with  $C_L$ .

Figure 5.- Comparison of the aerodynamic characteristics in pitch for the flat M-wing model and the flat arrow-wing model of reference 3.



(b) Variation of  $C_m$  with  $C_L$ .

Figure 5.- Continued.

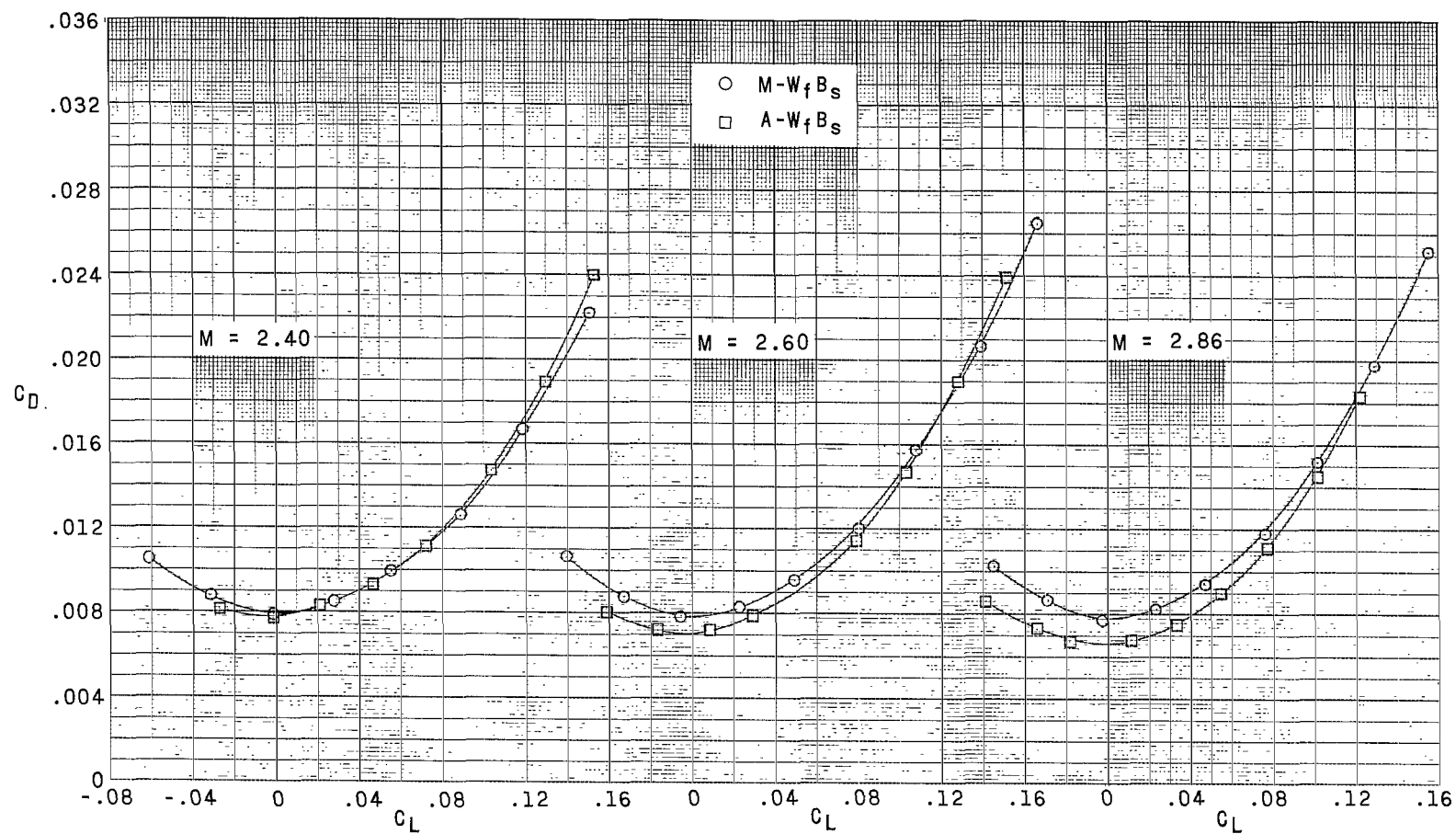
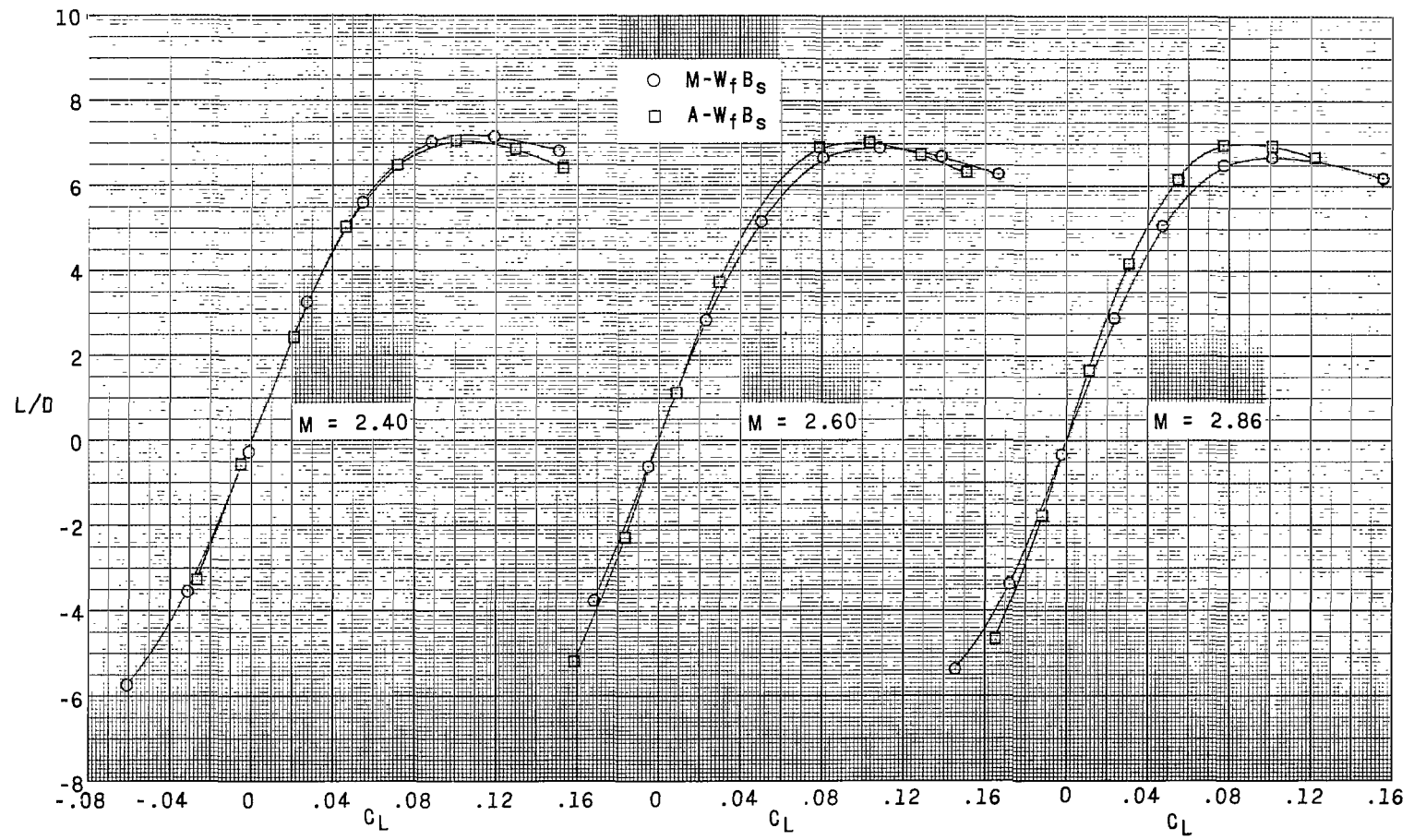
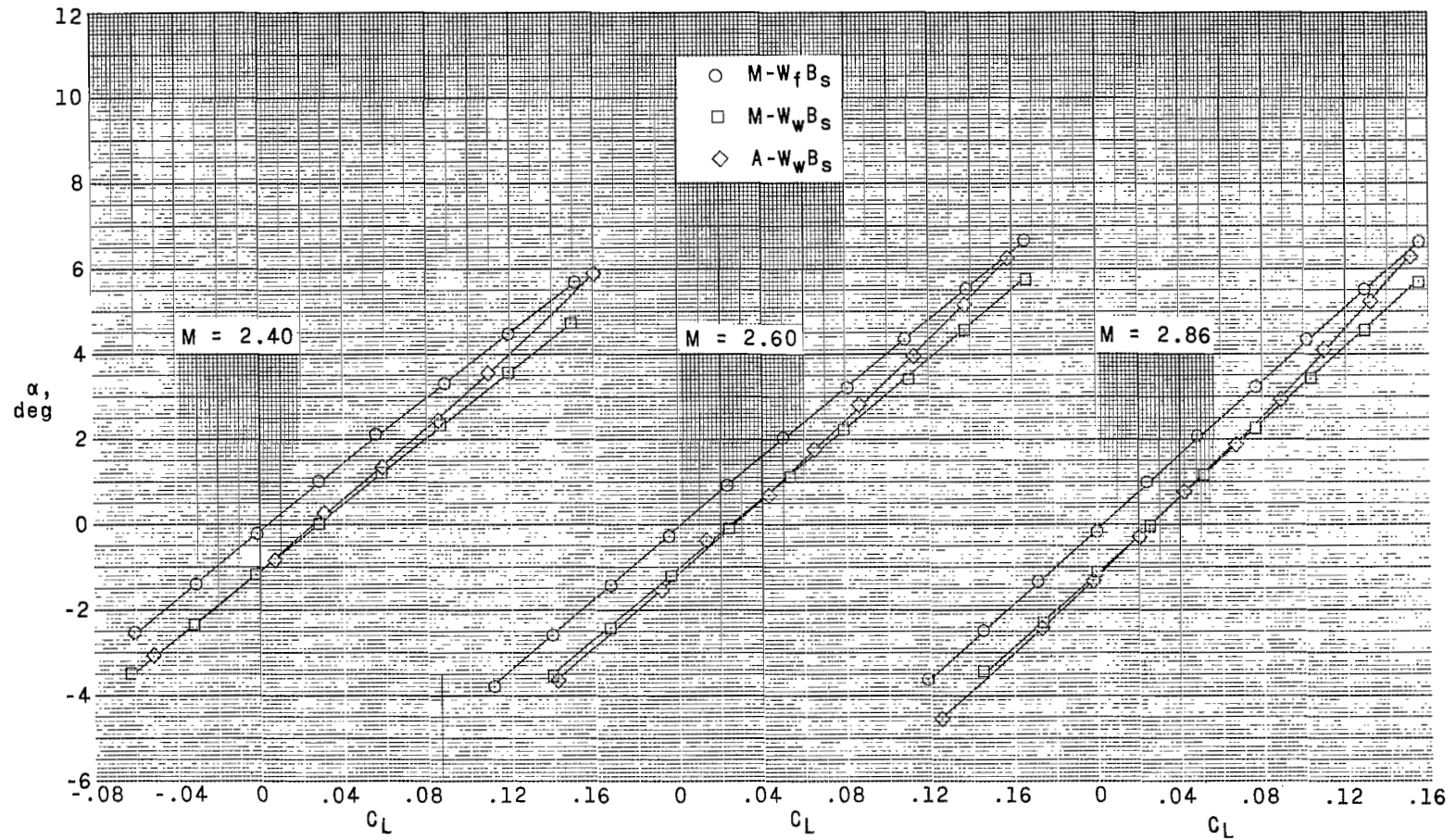
(c) Variation of  $C_D$  with  $C_L$ .

Figure 5.- Continued.



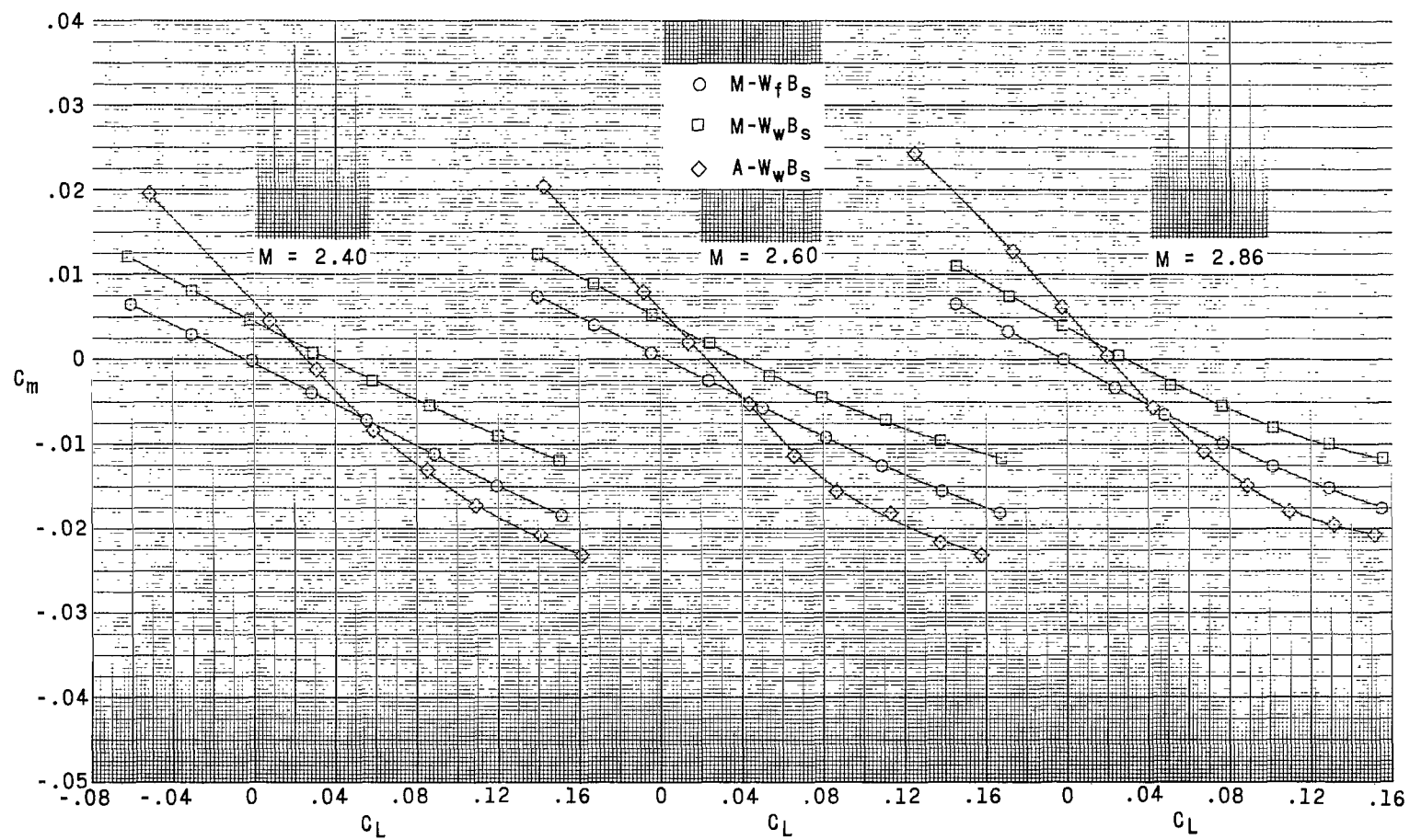
(d) Variation of  $L/D$  with  $C_L$ .

Figure 5.- Concluded.



(a) Variation of  $\alpha$  with  $C_L$ .

Figure 6.- Comparison of the aerodynamic characteristics in pitch for the flat M-wing model, the warped M-wing model, and the warped arrow-wing model of reference 3.



(b) Variation of  $C_m$  with  $C_L$ .

Figure 6.- Continued.

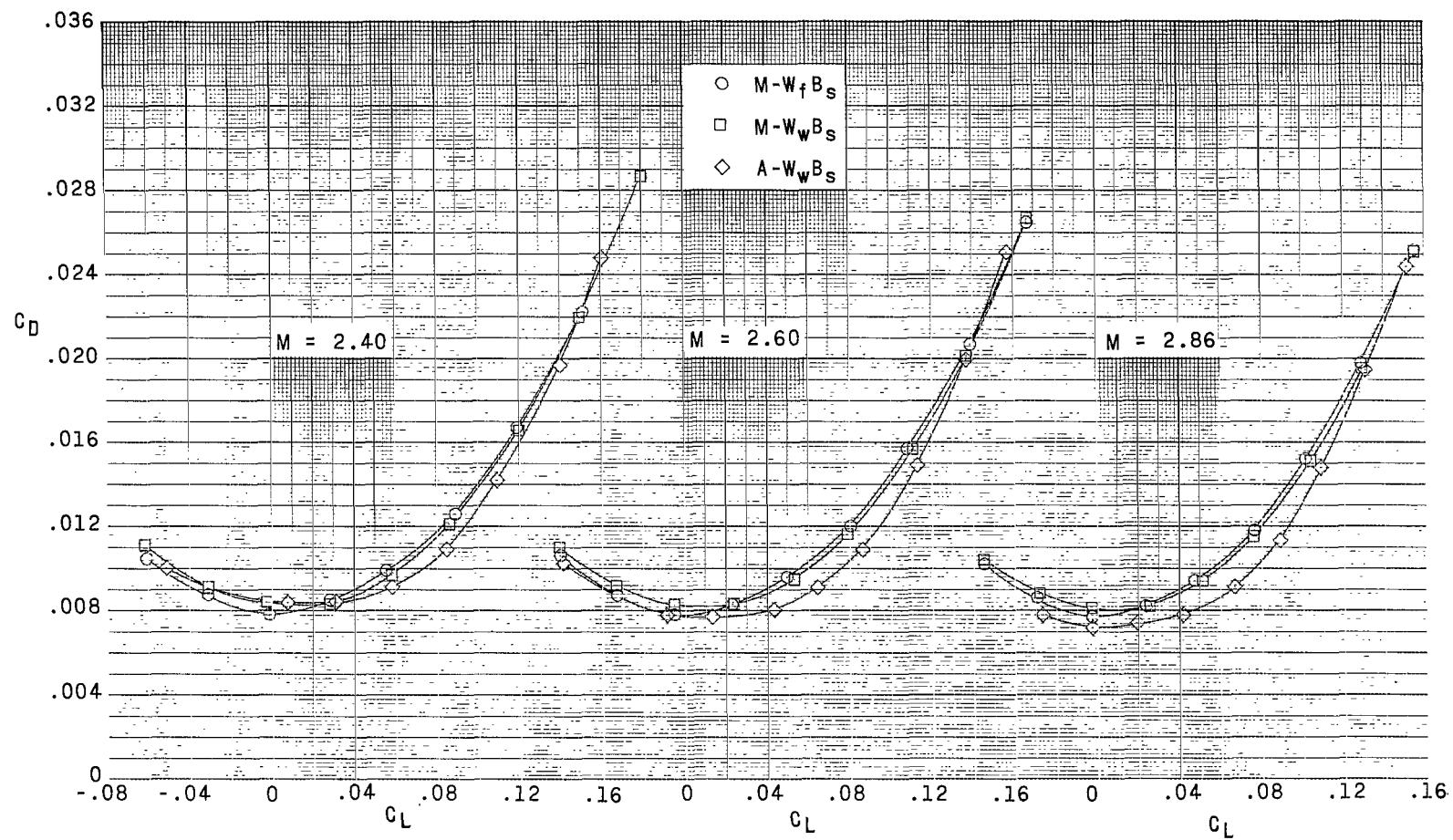
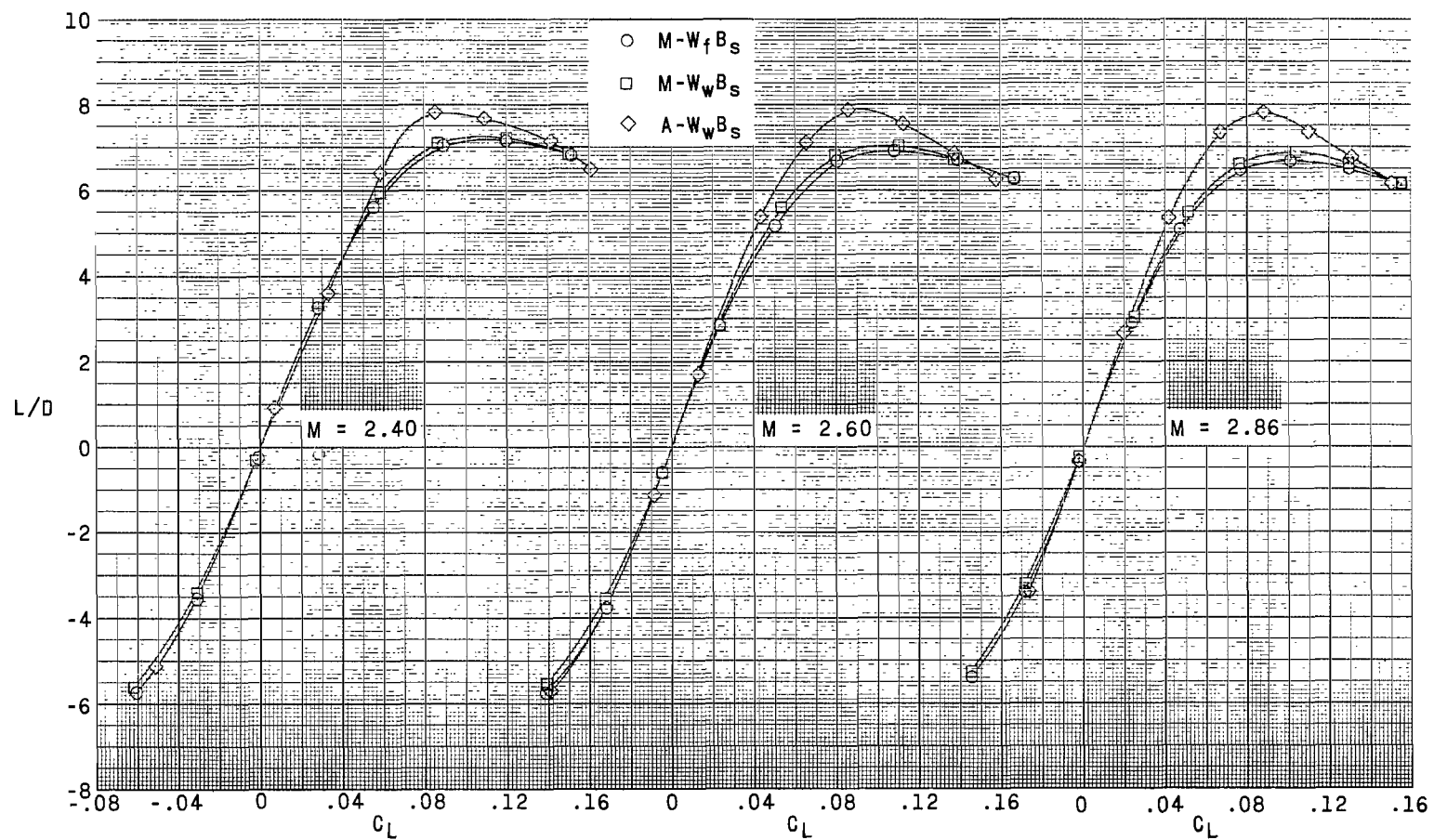
(c) Variation of  $C_D$  with  $C_L$ .

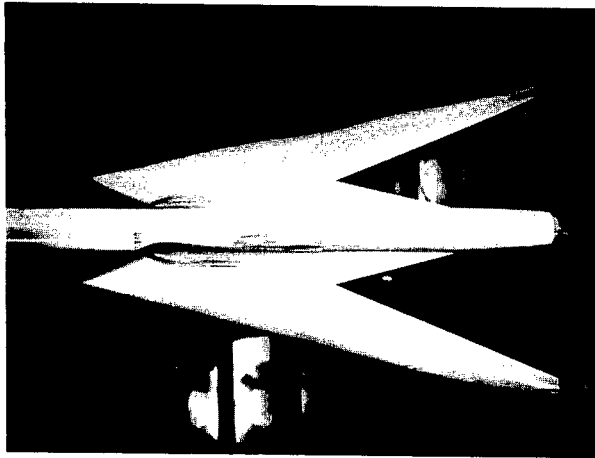
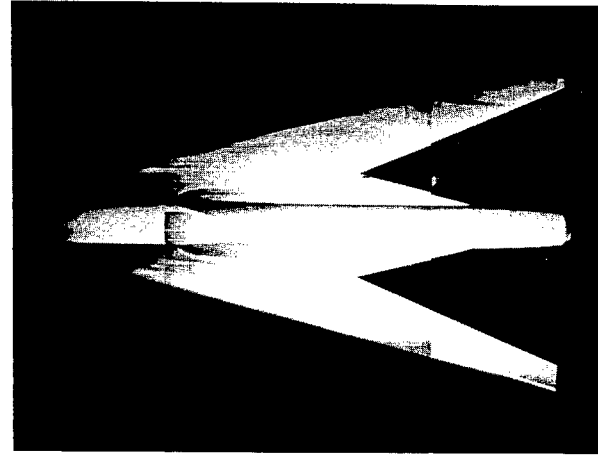
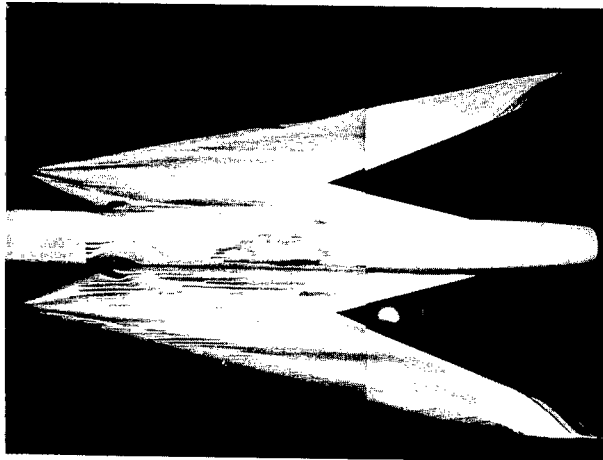
Figure 6.- Continued.



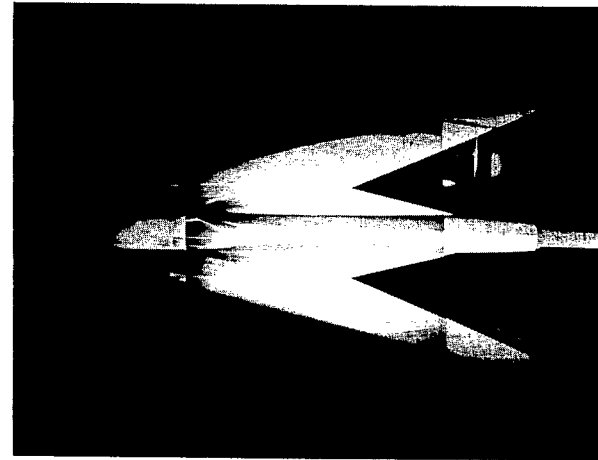
(d) Variation of  $L/D$  with  $C_L$ .

Figure 6- Concluded.




 $\alpha = 0^\circ$ 

 $\alpha = 0^\circ$ 

 $\alpha = 2.8^\circ$ 

(a) Wing upper surface.


 $\alpha = 2.8^\circ$ 

(b) Wing lower surface.

L-65-109

Figure 7.- Oil-flow photographs of warped M-wing model with long nose at  $M = 2.60$ .

3/13/25  
d

*"The aeronautical and space activities of the United States shall be conducted so as to contribute . . . to the expansion of human knowledge of phenomena in the atmosphere and space. The Administration shall provide for the widest practicable and appropriate dissemination of information concerning its activities and the results thereof."*

—NATIONAL AERONAUTICS AND SPACE ACT OF 1958

## NASA SCIENTIFIC AND TECHNICAL PUBLICATIONS

**TECHNICAL REPORTS:** Scientific and technical information considered important, complete, and a lasting contribution to existing knowledge.

**TECHNICAL NOTES:** Information less broad in scope but nevertheless of importance as a contribution to existing knowledge.

**TECHNICAL MEMORANDUMS:** Information receiving limited distribution because of preliminary data, security classification, or other reasons.

**CONTRACTOR REPORTS:** Technical information generated in connection with a NASA contract or grant and released under NASA auspices.

**TECHNICAL TRANSLATIONS:** Information published in a foreign language considered to merit NASA distribution in English.

**TECHNICAL REPRINTS:** Information derived from NASA activities and initially published in the form of journal articles.

**SPECIAL PUBLICATIONS:** Information derived from or of value to NASA activities but not necessarily reporting the results of individual NASA-programmed scientific efforts. Publications include conference proceedings, monographs, data compilations, handbooks, sourcebooks, and special bibliographies.

*Details on the availability of these publications may be obtained from:*

SCIENTIFIC AND TECHNICAL INFORMATION DIVISION  
NATIONAL AERONAUTICS AND SPACE ADMINISTRATION  
Washington, D.C. 20546